Methane emissions show recent decline but strong seasonality in two US Northeastern cities

Anna Karion[1*], Subhomoy Ghosh[1,2+], Israel Lopez-Coto[1,3], Kimberly Mueller[1], Sharon Gourdji[1++], Joseph Pitt[3,4] and James Whetstone[1]

[1] Special Programs Office, National Institute of Standards and Technology, Gaithersburg, MD, 20899
[2] Center for Research Computing, University of Notre Dame, South Bend, IN, 46556
[3] School of Marine and Atmospheric Sciences, Stony Brook University, Stony Brook, NY, 11794
[4] School of Chemistry, University of Bristol, Bristol, UK, BS8 1QU

[+] Current affiliation: Thrasio, Walpole, MA, 02081
[++] Current affiliation: Moody's RMS, Newark, CA, 94560

[*]Corresponding author email: Anna.Karion@nist.gov

Abstract

Urban methane emissions estimated using atmospheric observations have been found to exceed estimates derived using traditional inventory methods in several northeastern US cities. In this work, we have leveraged a nearly five-year record of observations from a dense tower network coupled with a newly developed high-resolution emissions map to quantify methane emission rates in Washington, DC, and Baltimore, Maryland. Annual emissions averaged over 2018-2021 were 80.1 [95% CI: 61.2, 98.9] Gg in the Washington DC urban area and 47.4 [95% CI: 35.9, 58.5] Gg in the Baltimore urban area, with a decreasing trend of approximately 4 % to 5 % per year in both cities. We also find wintertime emissions 44 % higher than summertime emissions, correlating with natural gas consumption. We further attribute a large fraction of total methane emissions to the natural gas sector using a least squares regression on our spatially-resolved estimates, supporting previous findings that natural gas systems emit the plurality of methane in both cities. This study contributes to the relatively sparse existing knowledge base of urban methane emissions sources and variability, adding to our understanding of how these emissions change in time, and provides evidence to support efforts to mitigate natural gas emissions.

Keywords: methane, greenhouse gas, urban, emissions

Synopsis

Methane emissions from US cities often exceed inventory data. This study confirms this and further finds that emissions are 44% higher in winter than in summer in Washington DC and Baltimore, MD.

1. Introduction

To mitigate the worst effects of climate change, national governments have launched efforts to reduce their emission of climate-warming greenhouse gases (GHG), including carbon dioxide (CO_2) and methane (CH_4)[1, 2]. In addition to global and national efforts, state, local, and municipal governments have also pledged to ambitious GHG emissions reduction goals, often relying on inventory estimates of their GHG emissions to track progress[3]. Emissions of CH_4 may be less economically painful for some industries to mitigate than those of CO_2, and CH_4 emissions reductions may be able to provide some short-term benefits, reducing atmospheric warming in the near-term until more complete structural changes can be made to mitigate CO_2.

However, recent studies have indicated that many sources of urban CH_4 to the atmosphere are fugitive (i.e., unintentional) emissions from the natural gas and waste sectors and are under-estimated by traditional accounting methods. For example, Washington, D.C., and Boston, Massachusetts were two of the first cities whose streets were sampled using a mobile platform to identify natural gas distribution pipeline leaks[4-6], calling attention to the prevalence of this source of CH_4 emissions in cities. Additionally, cities across the US have been the focus of studies quantifying total CH_4 emissions using observations from both airborne and stationary platforms[7-15], including several studies in Washington, D.C. and Baltimore, Maryland[16-19]. These studies relied on atmospheric observations of CH_4, generally integrating the contributions of all emissions sources together. As such, atmospheric methods are less precise in the spatial allocation of emissions sources than traditional accounting methods, but are also less prone to bias and can provide the means for verification of more traditional methods.

A few studies have suggested that post-meter emissions from residential and commercial natural gas consumers may comprise a significant portion of US CH_4 emissions[20-22]. Several of these measured natural gas leaks and emissions from household appliances, including furnaces, water heaters, and stoves[22-24], or entire single-family homes[21]. As a result, the US EPA has incorporated post-meter emissions for the first time in the most recent 2022 Greenhouse Gas Inventory[25]. To our knowledge, three top-down studies to date support the hypothesis that post-meter emissions may play an outsized role in US cities by finding higher emissions in winter, when natural gas consumption for heating is greater due to colder weather[8, 9, 26]. A recent study estimated that all natural gas emissions in Los Angeles were related to consumption with a very large wintertime increase, without attributing them to any specific part of the supply chain (e.g., pipelines or post-meter)[27].

In this study, we continue this line of atmospheric observation-based analyses to estimate CH_4 emissions from Washington, D.C. and Baltimore, Maryland for a nearly five-year period from May 2017 through December 2021. Our approach uses a dense network of tower-based CH_4 observations along with a custom emissions map within a Bayesian inversion framework to optimize emissions at a spatial resolution of 0.01 degrees. Our posterior results allow for a comparison of the two cities, as well as an investigation of the seasonal variability and trends in emissions over these years.

2. Methods

2.1. Domain, observations, and background

Our study focuses on the Census-designated urban areas[28] of Washington, D.C., and Baltimore, MD, two adjacent large metropolitan areas in the US Northeast (Fig. 1A). The Washington D.C. urban area (DC UA), with a population of approximately 4.6 million and land area of 3423 km^2, is significantly larger than the Baltimore urban area (Balt UA), at 2.2 million and 1857 km^2 (per the 2010 Census). There are nine landfills in the Balt UA (6 of which are closed), including two large active landfills (Alpha Ridge and Quarantine Road). Within the DC UA, all four landfills are closed. In both UAs, natural gas is widely used for residential and commercial heating. Wetlands in the domain are generally found outside the two UAs in the southeast of the modeling domain in the Eastern Shore area, although there are freshwater reservoirs and rivers (Potomac, Anacostia) and the Baltimore Harbor within the UAs.

We use CH_4 observations from the Northeast Corridor tower-based atmospheric concentration observing network from May 2017 to December 2021 in our analysis, with the number of urban stations varying between 6 and 11 through the time period as the network expanded[29, 30]. CH_4 dry air mole fractions (presented here as nmol mol^{-1}) are measured continuously by commercial cavity ring-down analyzers at approximately 0.4 Hz from two different heights on communications towers through the area. Here we use CH_4 observations from the tallest level, averaged hourly, as documented in detail in Karion et al[29]. Our network was designed specifically to maximize coverage of the Baltimore and Washington DC urban regions[31] with observations from three additional sites near the edges of our modeling domain used to determine the background conditions[32] (Fig. 1 and Supplementary Information (SI) Table S1). We use hourly-averaged observations during local afternoon hours, defined as between 5 hours after local sunrise and before sunset (SI Figs. S1 and S2). Our analysis relies on CH_4 enhancements caused by emissions within the modeling domain, around the DC and Balt UAs (Fig. 1A). In order to isolate the urban enhancements, the background mole fraction of CH_4 entering the domain must be removed from the total CH_4 measured at the urban sites. Here we use two different background determination methods that were found to be unbiased at monthly scales in a previous analysis[33], with details in SI Section S1.

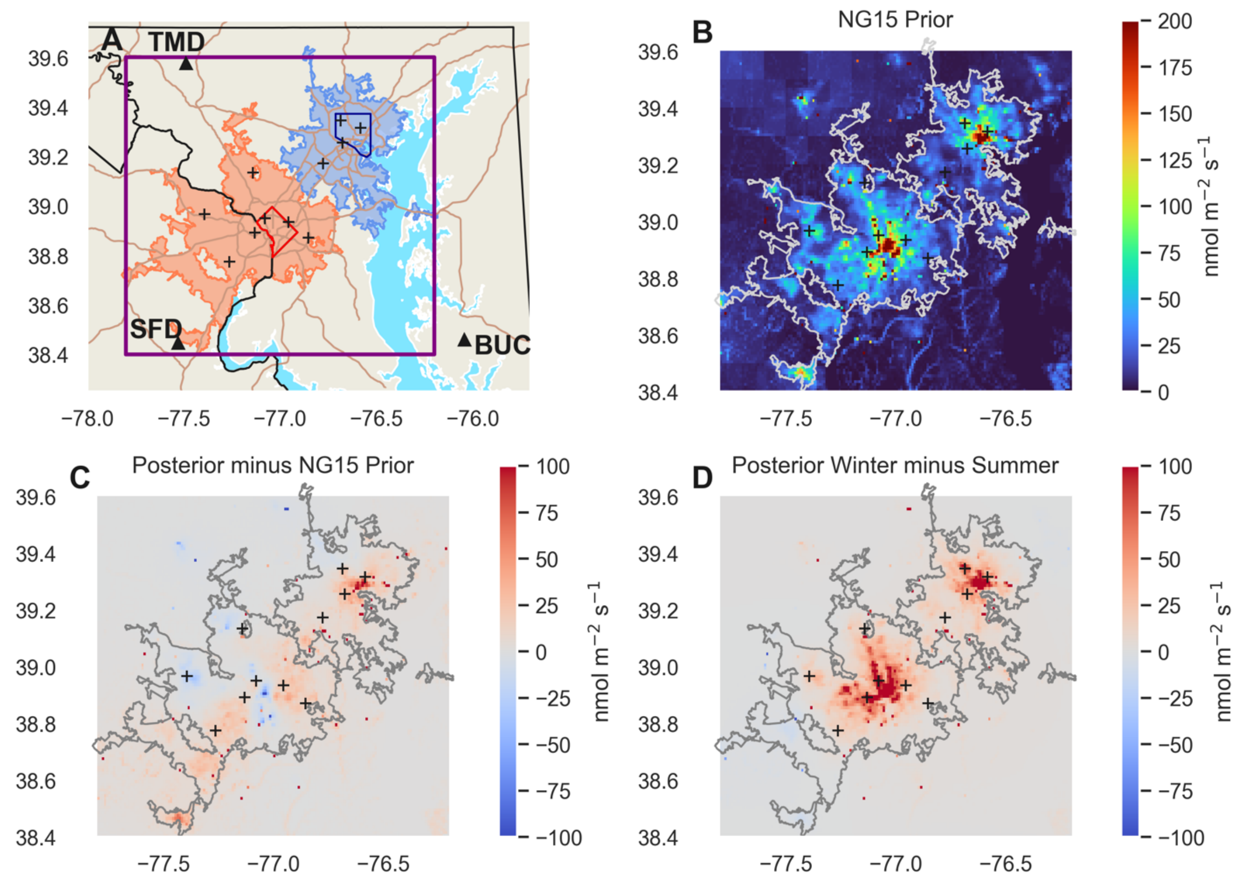

Fig. 1. Spatial representations of domain and results. (A) Map of modeling domain (purple outline), including highways (brown), the city of Washington, D.C. (red outline, with census-designated urban area (DC UA) in orange shading), the city of Baltimore, Maryland (blue outline, with urban area (Balt UA) in lighter blue shading), urban tower locations (+), and background tower locations (triangles). (B) CH_4 emissions of our prior flux (version NG15 (SI Appendix S3 and Table S6)); color scale maximum has been truncated to 200 nmol $m^{-2}s^{-1}$ for visibility. (C) Mean posterior emissions difference from the NG15 prior. (D) Mean winter posterior emissions difference from summer posterior. Balt and DC UAs are outlined in white or gray in (B-D).

2.2. Transport modeling

We use six different transport model configurations in the analysis. All configurations use the Stochastic Time-Inverted Lagrangian Model [34] (STILT) to simulate transport and dispersion, driven by meteorological fields from three models: North American Mesoscale (NAM), ECMWF Re-Analysis (ERA 5) [35], and the Weather Research and Forecast (WRF) model [36](SI Table S2). STILT was run with and without a near-field correction for each meteorological model (SI Section S2). The footprints provide good coverage over the urban areas for each year (SI Fig. S3), with similar coverage in winter (DJF) and summer (JJA) (SI Fig. S4). Notably, winter footprints are stronger overall than summer, reflecting generally shallower mixing height in winter.

2.3. Prior emissions map

As part of our modeling framework, we developed several versions of a custom high-resolution (0.01°, i.e., gridded at approximately 0.86 km by 1.11 km) emissions map based on methods developed by Pitt et al. [37] to use as priors (Fig. 1B). This emissions map, which is time-invariant, provides the Bayesian inversion system the best chance of estimating emissions at high resolution. The prior covers our geographical modeling domain, bounded by 38.4°N, 39.6°N, 77.8°W, and 76.2°W.

We have included nine sectors in our prior emissions map. Broadly, these are: natural gas (NG) distribution, NG transmission, landfills, wastewater, composting, mobile and stationary combustion, agriculture (manure management and enteric fermentation), and wetlands (including freshwater features). The NG distribution sector is the largest component of the prior, and itself has two components which were summed: an estimate of emissions using traditional EPA methodology[38] with some emission factors also from Weller et al. [39], and an estimate of additional loss on residential and commercial annual consumption (0.5% to 1.5%). Landfill emissions are the second largest sector, with emissions for most derived from the EPA's greenhouse gas reporting program (GHGRP[40]). Additional detail on all sectors is provided in SI Section S3, SI Figs. S5-S7, and SI Tables S3-S5. A comparison of our priors with the 2012 gridded EPA inventory[41] indicates that our priors are higher than the EPA inventory in the urban areas, with generally higher NG emissions and lower landfill emissions (SI Fig. S6).

We use five different versions of this prior for our set of inversions (SI Table S6), all based on the initial emissions map but altering the magnitudes of some sectors in each to better assess the impact of plausible choices made and uncertainties in the emission factors. We use three different options for a natural gas (NG) loss rate, as well as one prior with three times the emissions from waste and one with tripled wetlands emissions. Since the priors are constant in time, the seasonality and trend in our posterior are not driven by changes in prior emissions.

2.4. Inverse model

CH_4 fluxes are estimated with a Bayesian inversion system at 0.01° resolution in the domain shown in Fig. 1 for the period from May 2017 through December 2021. Inversions are performed every 10 days with a 5-day overlap between consecutive inversions, with emissions assumed to be constant in time over each 10-day inversion period. The following equations are used to solve for both the posterior fluxes $\hat{\boldsymbol{x}}$ and their corresponding posterior uncertainties, $\boldsymbol{A}$ [42]:

$$\hat{\boldsymbol{x}} = \boldsymbol{x_b} + \boldsymbol{BH^T}(\boldsymbol{HBH^T} + \boldsymbol{R})^{-1}(\boldsymbol{y} - \boldsymbol{Hx_b}) \quad \textbf{(1)}$$

$$\boldsymbol{A} = \boldsymbol{B} - \boldsymbol{BH^T}(\boldsymbol{HBH^T} + \boldsymbol{R})^{-1}\boldsymbol{HB} \quad \textbf{(2)}$$

In the formulation above, $\boldsymbol{x_b}$ is the prior flux, $\boldsymbol{B}$ represents the prior error covariance matrix, $\boldsymbol{H}$ is the sensitivity matrix, i.e., the matrix of footprints, $\boldsymbol{R}$ is the model-data mismatch covariance matrix, and $\boldsymbol{y}$ represents the vector of observed enhancements after the background mole fraction has been subtracted from the observations. SI Section S4 provides details on the construction of $\boldsymbol{B}$ and $\boldsymbol{R}$**,** inversion metrics, and uncertainties (SI Figs. S8 and S9). Posterior fluxes are aggregated to the Census-designated urban area (UA) for each of the two cities and averaged monthly. We explore the sensitivity of our results to the choice of observations in SI Section S5.1 and SI Fig. S10, and the sensitivity to the model-data mismatch covariance in SI Section S5.2 and SI Fig. S11.

As in Huang et al. and Lopez-Coto et al. [18, 19], we adopt the approach of running multiple inversions with different plausibly correct configurations, i.e., meteorological fields, background conditions, and priors, and present the spread between them (60 configurations in our case) as an estimate of uncertainty. Details of the configurations (summarized in SI Table S7) and their impact are found in SI Section S6 and SI Figs. S12 – S14. Inversions run to test sensitivities to model-data mismatch or number of observations are not included in the final ensemble.

2.5. Sectoral attribution of emissions

To attribute our emissions totals to different sectors, we first combine the nine sectors from our prior into three groups: Thermogenic (Mobile and Stationary Combustion, NG Transmission, NG Distribution), Biogenic-Waste (Landfills, Wastewater, Compost) and Biogenic-Wetlands&Ag (Wetlands, Agriculture). These three groupings provide maps that are spatially uncorrelated, and we estimate the contribution of each group to our total mean posterior for each season using a multiple linear regression to the prior maps of the groups, with no offset term. The regression is performed spatially, i.e., pixel-wise, with the total posterior map being regressed against the three explanatory variables, i.e., the three different maps (one for each grouping). We average posterior emissions for each inversion ensemble member for June, July, and August (JJA) of all years for summer, and for December, January, and February (DJF) for winter. As with the total posterior emissions, after estimating mean emissions from each group for each of the 60 inversions, we average them and use their spread to show confidence intervals with the results. We also calculate the thermogenic fraction as the fraction of total emissions attributable to the thermogenic group, for each of the 60 inversions (and for summer and winter seasons). The resulting estimated fractions are averaged with their distribution used to derive the 95% CI on the mean value. SI Section S8 shows additional details of the method, along with the dependence of the thermogenic fraction on the prior (SI Fig. S16).

2.6. Analysis of relationship to natural gas consumption

To estimate natural gas (NG) use in the two UAs, we spatially downscale NG consumption data reported by the local distribution companies [43] (LDCs, SI Fig. S5) in the region using gridded residential and commercial CO_2 emissions from Vulcan 3.0 [44, 45] assuming that gas use spatially scales with on-site combustion of natural gas and oil. We downscale temporally to monthly consumption using reported state-level monthly commercial and residential NG consumption for Maryland as a proxy [46]. We perform an ordinary least squares regression between monthly posterior emissions and estimated NG usage in each UA for each inversion ensemble member and report the mean slope and confidence intervals (SI Fig. S13 shows the impact of inversion configuration on the slope).

3. Results and Discussion

3.1. Urban area totals and spatial distribution of emissions

Aggregating the posterior emission rate of CH_4 over the Baltimore urban area (Balt UA) and the Washington DC urban area (DC UA), we report mean emissions for each over the entire period (Fig. 2; impact of model configuration in SI Fig. S12). Mean posterior estimates are generally consistent with previous estimates for this region [16, 17, 47], and slightly lower than the City of Baltimore inventory (SI Section S7 and SI Figs. S15 and S18). The spatial distribution of posterior emissions and the difference from the NG15 prior indicates an adjustment of emissions downward in the center of DC UA, but upwards around downtown Baltimore (Fig. 1C). Some areas to the northwest of both UAs in the farther suburbs are also adjusted downward.

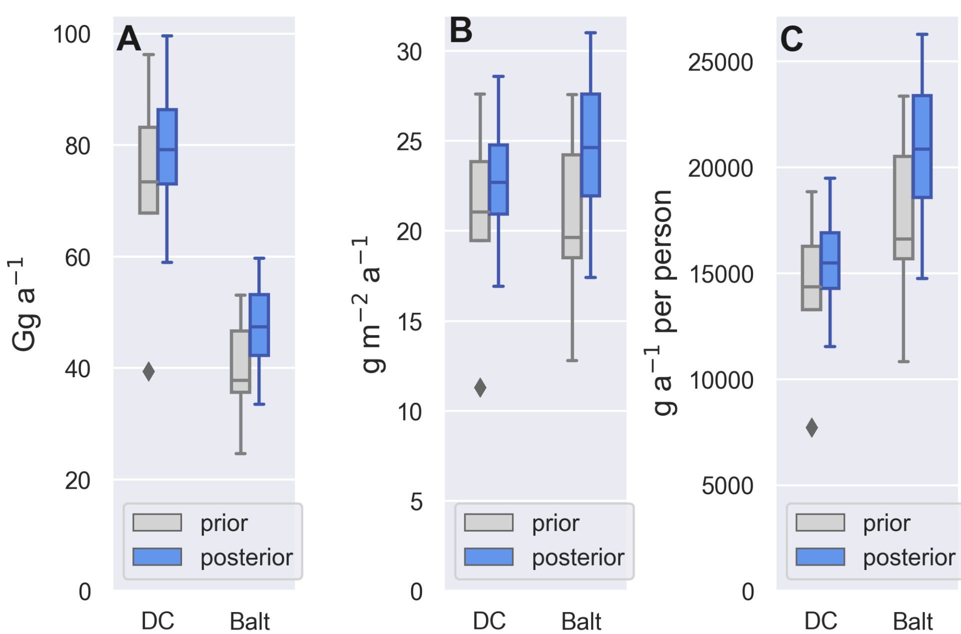

Fig. 2. Estimated total emission rate (average over the study period) for each UA (A), normalized by area (B) or per capita (C). Box plots indicate the spread across priors and posteriors for the set of inversions. The box edges indicate the quartiles of the dataset while the whiskers extend to show the rest of the distribution, except for points determined to be outliers which are shown as diamonds.

A comparison of total emissions, averaged over the entire study period, between the two UAs suggests slightly higher posterior emissions in the Balt UA than the DC UA per unit area and significantly higher emissions per capita (Fig. 2; SI Section S7 for methods). Our priors also contain larger per capita emissions in the Balt UA, with the difference between the two areas dominated by landfill emissions; the Balt UA contains more landfills within its boundary than DC. This example illustrates that emissions comparisons, even after normalizing by area or population, sometimes come down to a specific domain definition. For example, the Brown Station Landfill in Prince George's County, MD, a suburb of Washington DC, lies one grid cell outside our DC UA, although it serves the DC UA's population. Thus, a more in-depth examination or interpretation of the drivers of differences in cities' emissions should include Scope 2 and Scope 3 emissions (i.e., including emissions that occur outside the UA due to activity within the area). Bottom-up inventories conducted by localities and metropolitan areas, including those of Baltimore and Washington, D.C., generally include Scope 2 and sometimes Scope 3 out-of-area emissions, and differences in Scope remain one challenge in robustly comparing bottom-up inventories with top-down analyses [48].

3.2. Seasonality of emissions

The mean emissions from our inversions indicate distinct seasonality in total CH_4 emissions in both cities, with emissions 1.44 times higher in winter than in summer (Fig. 1D). Spatial differences between the seasons suggest more wintertime emissions in both core downtown areas with the highest density of population, buildings, and natural gas usage. Higher wintertime emissions have been found in previous studies in Boston [8] and Los Angeles [9], as well as in the Washington DC and Baltimore region [18]. In those studies, the higher winter emissions were attributed to NG leakage, possibly post-meter. Here we also find a strong correlation in our monthly posterior emissions estimates with residential and commercial natural gas use in both UAs ($R^2 = 0.52$ in the DC UA and $R^2 = 0.42$ in the Balt UA) (Fig. 3). We discuss this relationship further in Section 3.4.

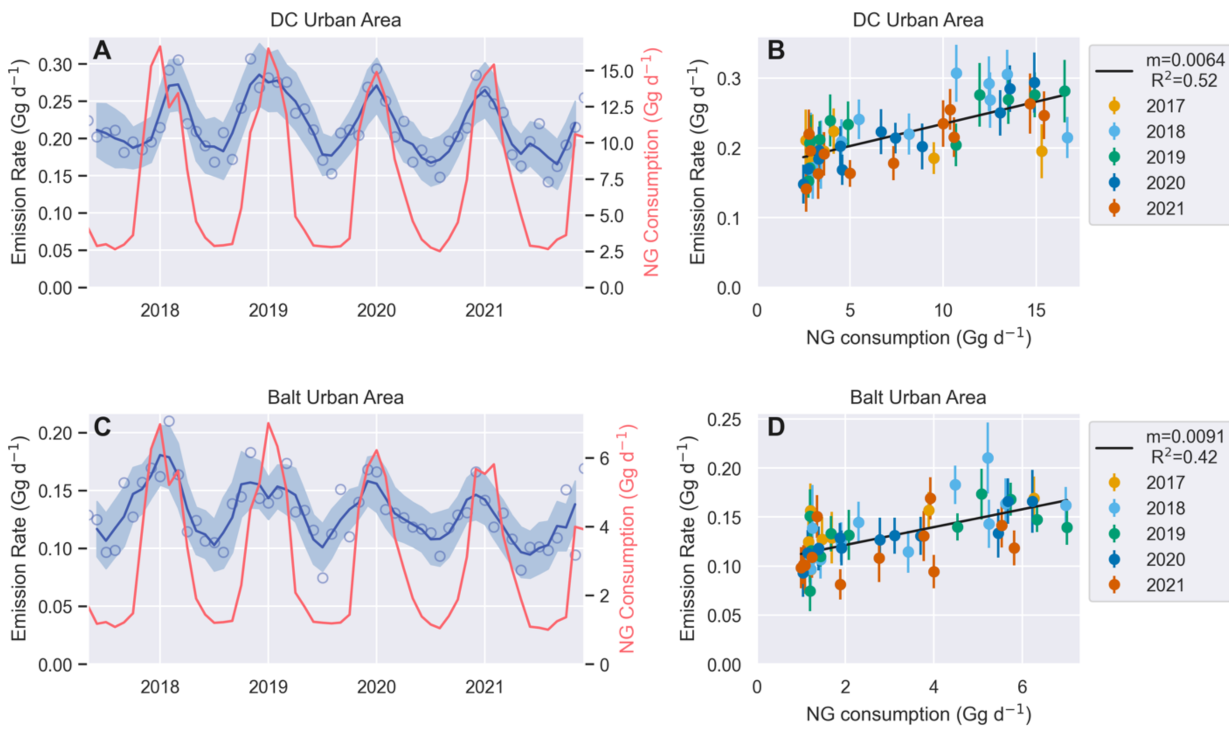

Fig. 3. (A, C): Urban area posterior mean monthly emission rate across inversions (blue circles); blue line and shading are the 3-month rolling mean and 3-month rolling mean standard deviation across inversions. Red line, corresponding with the right axis, indicates commercial and residential natural gas consumption estimated in each UA (see text for methods). (B ,D): Monthly mean emission rate colored by year as a function of residential and commercial gas consumption in each UA. Error bars on monthly emission rates are the standard deviation across inversions. Line shows mean fit, with slope as indicated in the legend.

3.3. Sectoral distribution of emissions

A multivariate linear regression analysis using our customized high-resolution priors separated by sector groupings (Thermogenic, Biogenic-Waste and Biogenic-Wetlands&Ag) provides some understanding of the sources of emissions in the two UAs in winter and summer.

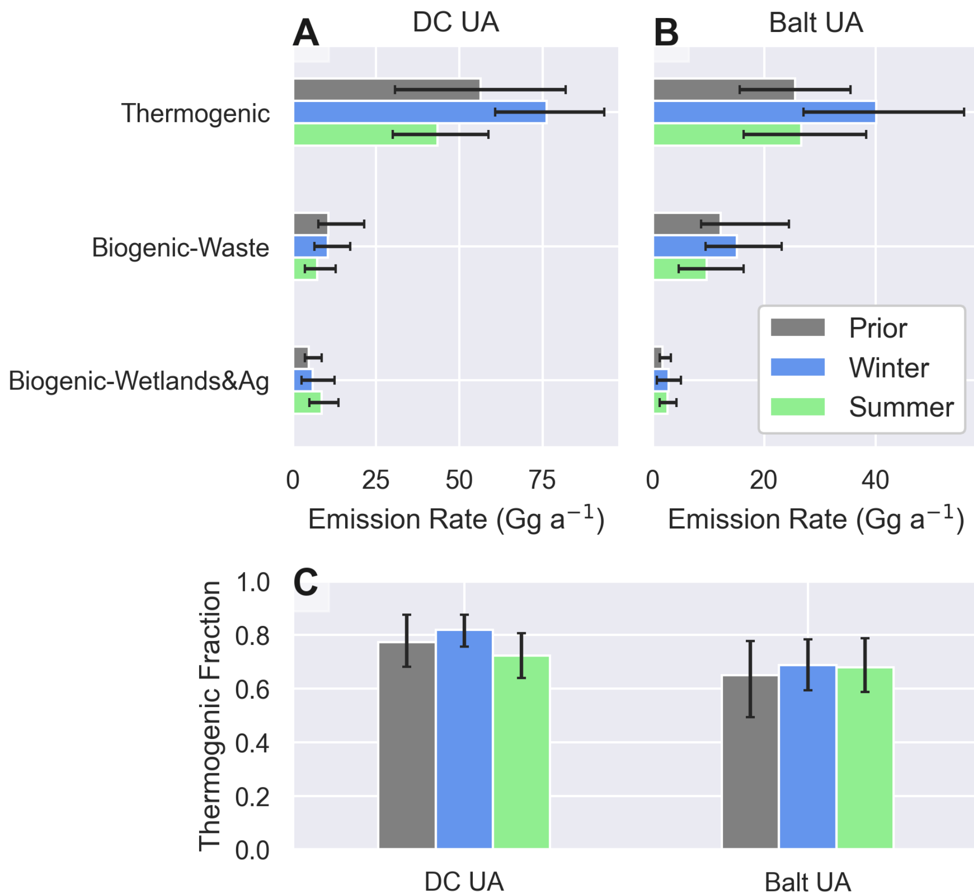

Fig. 4. Estimated sector-grouped emissions for DC (A) and Balt (B) for the mean of the priors, the posterior mean for winter and summer. (C) Estimated thermogenic fraction of emissions for the each UA. Legend in (B) applies to all three panels; error bars represent the 95% CI based on the ensemble of inversions.

Our results suggest that thermogenic emissions from fossil-fuel combustion and NG losses are higher in winter than in summer, supporting the hypothesis that overall emissions seasonality is driven by the NG sector. Interestingly, waste emissions are also higher in winter than in summer in both UAs. This result follows from the spatial allocation of the winter-summer difference (Fig. 1D) along with the spatial allocation of NG distribution and landfill emissions in the priors. In this analysis, it is likely that the spatial overlap of large landfills within the same areas with large NG emissions does not allow for this methodology to adequately distinguish between these two sources, and results in both NG emissions and landfill emissions being higher in winter. Possible seasonality in landfill emissions is discussed further in Section 3.4. Wetlands and agriculture are slightly higher in summer than in winter in DC, although not significantly so (Fig. 4).

We note that these results are necessarily dependent on the spatial allocation and relative magnitudes of these sector groups in the prior, both because of the general posterior dependence on the spatial map of the prior, but also because we are using a linear regression to scale each group, which does not account for posterior changes in the spatial distribution of emissions within a group. Therefore, we emphasize that a high-quality emissions map is crucial for using this method to attribute emissions to sectors.

Given the estimates of sectoral distribution of posterior emissions, we can determine the thermogenic fraction: the fraction of emissions from thermogenic sectors (NG distribution, NG transmission, mobile combustion, and stationary combustion) (Fig. 4C). In the Balt UA, the thermogenic fraction is 0.68 [95% CI: 0.59, 0.79] and 0.69 [95% CI: 0.59, 0.78] in summer and winter, respectively; in DC it is 0.73 [95% CI: 0.64, 0.81] and 0.82 [95% CI: 0.76, 0.88]. Baltimore's fraction is lower than DC's because there are more landfills within the Balt UA. When calculating this fraction for the entire model domain, the fractions fall to 0.50 [95% CI: 0.40, 0.62] in summer and 0.58 [95% CI: 0.48, 0.70] in winter, as would be expected since in our model most thermogenic emissions occur within the urban centers. We note that although our posterior sectoral distribution is closely correlated with the prior, the thermogenic fraction does change slightly from the prior value (Fig. 4C and SI Fig. S16), and varies marginally by season, indicating that our observations are able to inform this analysis beyond our prior attribution.

We did not expressly include emissions from either sewer leaks or wood burning in our prior – both sectors are likely to be spatially allocated similarly to NG distribution or post-meter emissions and would thus not be able to be distinguished using our methods. Using literature-based estimates of annual emissions from these two sources (SI Sections 3.3 and 3.5), we calculate that if they were both attributed to biogenic rather than thermogenic sectors, the thermogenic fractions would decrease to 0.68/0.79 (summer/winter) in the DC UA and 0.64/0.66 in the Balt UA, values that are within our uncertainty estimates.

Our estimated thermogenic fractions are generally consistent with previous measurements for these UAs based on ethane to methane ratios, although direct comparisons are difficult given the spatial disparity between the different studies. This suggests that our analysis using a combination of a custom prior and atmospheric observations may inform sectoral attribution without using a co-tracer, although not as definitively. Floerchinger et al. [26] estimated fractions of 0.26-0.30 and 0.63-0.69 in summer and winter, respectively, over the DC/Balt domain. The winter values correspond well with ours while their summer estimates are significantly lower than our values, even when we consider the entire domain. We suspect that their summer flight may have had significant river and wetland influence, and it could be that our tower network is not sensitive enough to fluxes outside the urban areas, minimizing our estimate of those biogenic emissions (either agricultural or natural). Plant et al. [17] also estimated the thermogenic fraction for the Balt UA (0.92) and DC UA (0.80) in spring 2018, values better aligned with our winter estimates for the UAs. In general, direct comparisons of the thermogenic fraction are subject to difficulties from spatial misalignment. The balance of sources differs between the denser urban areas and the surrounding regions, so that the mix of sources observed varies depending on the specific area sampled by an observation.

3.4. Relationship between emissions and natural gas use

Analyzing the monthly posterior emission rate and NG consumption in each UA, we estimate the slope of their relationship, i.e., the emission rate per unit NG consumed (Fig. 3B and Fig. 3D). The slope is slightly greater in the Balt UA (0.9 [95% CI: 0.6, 1.3] %) than it is in DC UA (0.6

[95% CI: 0.4, 0.9] %), indicating a slightly higher rate of emission in Balt than in DC per unit gas consumed, although the overlapping uncertainties on each indicate that this difference is not significant at the 95% CI. For comparison, Sargent et al. [8] reported a relationship of 2.1 % between NG emissions in Boston and NG use in the state of Massachusetts on a per unit area basis. This rate is not directly comparable to our finding because we have scaled NG use specifically for our UAs, and using state average NG use per unit area would yield a higher percentage. He et al. [9] found a slope of 1.4 % ± 0.1 % total CH_4 emissions per unit of residential and commercial NG use in the LA basin, while Zeng et al. [27] recently reported 2.8 % ± 0.18 % using the same methods over a longer time frame. These values are significantly larger than those we find in the DC and Balt UAs. Further investigation of emissions in both cities would be required to determine the source of these large differences, along with an analysis of the differences in infrastructure, both at the LDC and building and appliance level.

We note that the emission rate of 0.6 % and 0.9 % of NG use does not represent the overall loss rate of NG in the UAs; it represents only the component of emissions that varies according to NG consumption. The intercepts in the relationship between emissions and NG use represent 78 % to 79 % of total emissions in each UA, and only 21 % to 22 % vary with NG consumption. Given the thermogenic fractions measured by other studies[17, 26], additional NG losses that do not directly vary with NG use (e.g., system leaks that exist regardless of usage) also contribute to total emissions. Conversely, it is possible that some other emissions source is also higher in winter than in summer and contributes to the seasonal variability, as discussed below.

The second largest contributor to urban emissions in our priors is the landfill sector, and therefore it is the most likely (after NG distribution) to affect the seasonal variation in overall emissions at such a large scale. While landfill emissions can be seasonal, due to the dependence of CH_4 production, diffusion rates, and oxidation rates on soil temperature and moisture [49, 50], most inventory methods generally do not assign any seasonality to landfill emissions [41]. Variability in landfill emissions to the atmosphere has been found to depend largely on specific practices and operations (such as type of cover material or changes in landfill infrastructure) in addition to local climate and weather, including barometric pressure [51, 52]. The various emissions drivers compete and the overall dependence of net emissions on season depends on the specific location and practices at a given landfill. We would advocate for future work to focus on understanding of waste sector emissions, but accurate emissions estimates will likely require specific information on the individual landfills in question in order to model emissions and their variability properly.

Other biogenic sectors, such as wastewater (including from sewers) and wetlands, are unlikely to drive higher wintertime emissions. Wastewater and wetland emissions are generally higher in summer, due to greater methanogenic activity at warmer temperatures [53-55]; any seasonality would show higher summer emissions, so we do not expect these sectors to be contributing to the higher wintertime emissions observed.

We conclude that the most likely source of the higher winter emissions in the DC and Balt UAs is NG-related leakage from the distribution network and related infrastructure and/or post-meter emissions (these could include both leakage within buildings and incomplete combustion). Distribution networks may emit more in winter if pipes are maintained at higher pressures in winter to meet demand, but such pressure data is not publicly available and we do not have any other evidence of this. While Fischer et al.[21] found significant post-meter leakage from quiescent sources (i.e. not directly related to usage), they suggest that transient emissions may also play a large role, as has been found in other studies, leading to higher losses with more frequent usage [22, 24]. Therefore, we cannot determine definitively to what extent either distribution network or post-meter losses cause the seasonal variability found here.

3.5. Inter-annual variability and trend of emissions

An analysis of the annual average posterior emissions over time indicates a declining trend in both UAs from 2018 to 2021 (Fig. 5). We exclude the partial 2017 year from this analysis, as the average from May to December is not representative of an annual mean given the strong seasonality we have observed. We calculate the trend for each inversion configuration separately, to understand the influence of the configuration on the result (SI Fig. S14) and characterize the uncertainties using the spread across the inversion configurations. Our estimates of the decline in each UA are -3.6 [95% CI: -5.2, -1.8] Gg a^{-1} in DC and -2.8 [95% CI: -3.5, -2.2] Gg a^{-1} in Balt. These declines represent approximately 4.2 [95% CI: 6.1, 2.1] % and 5.4 [95% CI: 6.8, 4.3] % of 2018 average annual emissions per year in DC and Balt, respectively. In addition, we note here that contrary to emissions of CO_2[56], CH_4 emissions do not show any observable anomaly during 2020, when the COVID-19 pandemic-induced slowdown in economic activity occurred, although such a signal may have been obscured by other sources of variability.

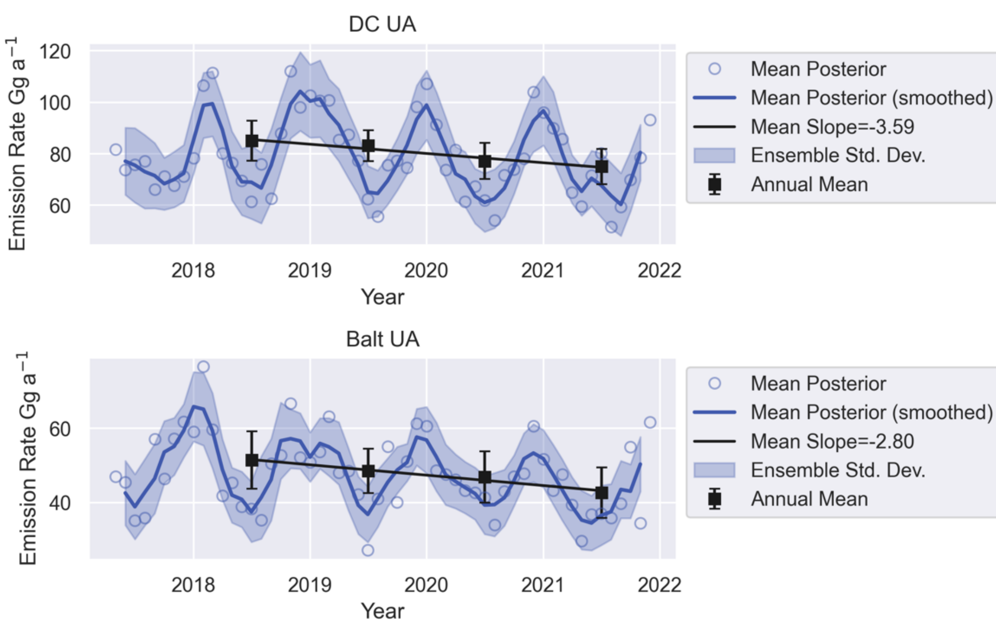

Fig. 5. Trend in annual mean CH_4 emissions. Circles are mean monthly emissions for the DC UA (A) and Balt UA (B), with the 3-month smoothed emissions indicated by solid lines, and squares indicating the annual means beginning with the first whole calendar year, 2018. Shading and error bars indicate the standard deviation across inversions. Slope indicated in the legend is the mean of the slopes across inversions.

Given our results correlating emissions to NG use, we also investigate the trend in NG consumption in our two UAs, to determine whether reductions in gas use could explain the decrease in emissions. Considering 2018-2021, residential and commercial NG consumption in the DC and Balt UAs declined by approximately 3 % and 6 % per year on average, respectively, according to data reported by local distribution companies [43]. In Section 3.4 we determined that for every additional unit of CH_4 consumed from residential and commercial NG use above the minimum value, total emissions increased by 0.006 and 0.009 (in DC and Baltimore, respectively). Therefore, we would expect that a decrease in NG use would result in a corresponding decline in emissions. Other losses from NG systems that are not seasonally varying (such as distribution pipeline leaks, for example) are not directly proportional to consumption rates so would not decline when consumption drops. Given the proportionality of emissions to NG use found in Section 3.4, the reductions in NG use would lead to CH_4 emissions declines of 0.31 Gg a^{-1} to 0.69 Gg a^{-1} in DC and 0.42 Gg a^{-1} to 0.90 Gg a^{-1} in Baltimore (ranges consider the 95% CI on the relationship between NG use and emissions). Therefore, while reductions in NG use likely contributed to some of the observed decrease in emissions (6 % to 38 % in DC and 12 % to 41 % in Baltimore), other factors also played a large role. These findings are further supported by an analysis calculating separate trends from warmer months and cooler months (SI Section S9). This analysis indicates that while wintertime emissions showed larger relative declines than summer, emissions from both declined over time (SI Fig. S17).

3.6. Discussion of main findings

In this study we determine average CH_4 emission rates of 80.1 [95% CI: 61.2, 98.9] Gg a^{-1} in the Washington DC urban area and 47.4 [95% CI: 35.9, 58.5] Gg a^{-1} in the Baltimore urban area (mean of annual averages from 2018-2021). We also find emission rates that are 44 % higher in winter and correlated with NG consumption, with emissions of 0.6 [95% CI: 0.4, 0.9] % and 0.9 [95% CI: 0.6, 1.3] % of NG use in DC and Baltimore, respectively, over a baseline seasonally-invariant emission rate. Spatial patterns in our posterior estimates suggest that NG loss drives the seasonal variability, with wintertime emissions higher in the city centers.

Normalizing emissions by either area or population indicates a slightly higher emissions intensity in Balt relative to DC, consistent with the larger rate of emissions per unit of gas use. While our results point to a four-year declining emissions trend of approximately 4 % to 5 % per year in both cities, we are unable to attribute this entire trend to decreasing NG use. Future work will focus on extending the period of analysis to better examine both the relationship to gas use and trends over time. We expect that additional years of analysis will allow for a more robust trend detection by reducing the uncertainties associated with the observed trends. Additional measurements of other trace gas species that are emitted by NG leaks (e.g., ethane) and isotopes of CH_4 are also needed to better disentangle the various urban sources of CH_4 to the atmosphere.

Overall, our study contributes to the sparse existing knowledge base of CH_4 emissions in cities, adding valuable understanding of how these emissions change in time. Understanding the urban sources of CH_4 may enable policymakers from local to national levels better target mitigation efforts. Several municipalities have already passed legislation to limit new natural gas hookups, including Montgomery County, Maryland, which lies in our study area [57]. Some LDCs, including Baltimore Gas and Electric, have invested in repairing and upgrading NG distribution infrastructure (https://marylandstride.com/) to improve reliability and avoid critical failures while also reducing the GHG footprint of NG use, and it is possible that these improvements contributed to the observed emissions declines. This study provides evidence to support mitigation efforts aimed at reducing the loss of NG in urban areas, but additional information that could more specifically point to the source of NG emissions and their variability is needed to further guide investments and regulation. Specifically, future studies should be designed to provide even more granularity in emissions sector understanding to better inform inventory methods and track mitigation effort success.

4. Data availability and supporting information

Atmospheric methane observations used in this study are available at Karion et al. [30], https://doi.org/10.18434/mds2-3012.

Supporting Information: Additional details on methods for observations, transport, high-resolution prior map construction (including maps for each sector), inversion system setup, and sectoral attribution of emissions; results of sensitivity tests, impact of model choices, additional analysis of long-term trend, and comparison to the City of Baltimore inventory. (PDF)

5. Acknowledgements

The authors thank Elizabeth DiGangi, Steve Prinzivalli, Charlie Draper, Bryan Biggs, Ben Michalak, and Seth Baldelli (Earth Networks, Inc.) for observation network operation. The authors have no competing interests. This work was funded by the NIST Greenhouse Gas Measurements Program, including through grants 70NANB19H132 (University of Notre Dame) and 70NANB19H167 and 70NANB21H021 (Stony Brook University). Certain equipment, instruments, software, or materials are identified in this paper to specify the experimental procedure adequately. Such identification is not intended to imply recommendation or endorsement of any product or service by NIST, nor is it intended to imply that the materials or equipment identified are necessarily the best available for the purpose.

References

(1) United Nations Framework Convention on Climate Change (UNFCCC). The Paris Agreement. 2016. https://unfccc.int/sites/default/files/resource/parisagreement_publication.pdf?download (accessed 2023 April).

(2) European Commission and United States of America. *Global Methane Pledge*. Climage and Clean Air Coalition, 2021. https://www.ccacoalition.org/en/resources/global-methane-pledge (accessed 2023 April 7).

(3) C40 Cities. *C40 Cities*. 2023. www.c40.org (accessed 2023 April 7).

(4) Jackson, R. B.; Down, A.; Phillips, N. G.; Ackley, R. C.; Cook, C. W.; Plata, D. L.; Zhao, K. Natural Gas Pipeline Leaks Across Washington, DC. *Environ. Sci. Technol.* **2014**, *48* (3), 2051-2058. DOI: 10.1021/es404474x.

(5) Phillips, N. G.; Ackley, R.; Crosson, E. R.; Down, A.; Hutyra, L. R.; Brondfield, M.; Karr, J. D.; Zhao, K.; Jackson, R. B. Mapping urban pipeline leaks: Methane leaks across Boston. *Environmental Pollution* **2013**, *173*, 1-4. DOI: https://doi.org/10.1016/j.envpol.2012.11.003.

(6) Hendrick, M. F.; Ackley, R.; Sanaie-Movahed, B.; Tang, X.; Phillips, N. G. Fugitive methane emissions from leak-prone natural gas distribution infrastructure in urban environments. *Environmental Pollution* **2016**, *213*, 710-716. DOI: https://doi.org/10.1016/j.envpol.2016.01.094.

(7) McKain, K.; Down, A.; Raciti, S. M.; Budney, J.; Hutyra, L. R.; Floerchinger, C.; Herndon, S. C.; Nehrkorn, T.; Zahniser, M. S.; Jackson, R. B.; Phillips, N.; Wofsy, S. C. Methane emissions from natural gas infrastructure and use in the urban region of Boston, Massachusetts. *Proceedings of the National Academy of Sciences* **2015**, *112* (7), 1941-1946, Article. DOI: 10.1073/pnas.1416261112.

(8) Sargent, M. R.; Floerchinger, C.; McKain, K.; Budney, J.; Gottlieb, E. W.; Hutyra, L. R.; Rudek, J.; Wofsy, S. C. Majority of US urban natural gas emissions unaccounted for in inventories. *Proceedings of the National Academy of Sciences* **2021**, *118* (44), e2105804118. DOI: 10.1073/pnas.2105804118.

(9) He, L.; Zeng, Z.-C.; Pongetti, T. J.; Wong, C.; Liang, J.; Gurney, K. R.; Newman, S.; Yadav, V.; Verhulst, K.; Miller, C. E.; Duren, R.; Frankenberg, C.; Wennberg, P. O.; Shia, R.-L.; Yung, Y. L.; Sander, S. P. Atmospheric Methane Emissions Correlate With Natural Gas Consumption From Residential and Commercial Sectors in Los Angeles. *Geophysical Research Letters* **2019**, *46* (14), 8563-8571. DOI: https://doi.org/10.1029/2019GL083400.

(10) Yadav, V.; Verhulst, K.; Duren, R.; Thorpe, A.; Kim, J.; Keeling, R.; Weiss, R.; Cusworth, D.; Mountain, M.; Miller, C.; Whetstone, J. A declining trend of methane emissions in the Los Angeles basin from 2015 to 2020. *Environmental Research Letters* **2023**, *18* (3). DOI: 10.1088/1748-9326/acb6a9.

(11) Lamb, B. K.; Cambaliza, M. O. L.; Davis, K. J.; Edburg, S. L.; Ferrara, T. W.; Floerchinger, C.; Heimburger, A. M. E.; Herndon, S.; Lauvaux, T.; Lavoie, T.; Lyon, D. R.; Miles, N.; Prasad, K. R.; Richardson, S.; Roscioli, J. R.; Salmon, O. E.; Shepson, P. B.; Stirm, B. H.; Whetstone, J. Direct and Indirect Measurements and Modeling of Methane Emissions in Indianapolis, Indiana. *Environ. Sci. Technol.* **2016**, *50* (16), 8910-U8530, Article. DOI: 10.1021/acs.est.6b01198.

(12) Pitt, J. R.; Lopez-Coto, I.; Hajny, K. D.; Tomlin, J.; Kaeser, R.; Jayarathne, T.; Stirm, B. H.; Floerchinger, C. R.; Loughner, C. P.; Gately, C. K.; Hutyra, L. R.; Gurney, K. R.; Roest, G. S.; Liang, J.; Gourdji, S.; Karion, A.; Whetstone, J. R.; Shepson, P. B. New York City greenhouse gas emissions estimated with inverse modeling of aircraft measurements. *Elementa: Science of the Anthropocene* **2022**, *10* (1). DOI: 10.1525/elementa.2021.00082 (acccessed 12/23/2022).

(13) Jones, T. S.; Franklin, J. E.; Chen, J.; Dietrich, F.; Hajny, K. D.; Paetzold, J. C.; Wenzel, A.; Gately, C.; Gottlieb, E.; Parker, H.; Dubey, M.; Hase, F.; Shepson, P. B.; Mielke, L. H.; Wofsy, S. C. Assessing urban methane emissions using column-observing portable Fourier transform infrared (FTIR) spectrometers and a novel Bayesian inversion framework. *Atmos. Chem. Phys.* **2021**, *21* (17), 13131-13147. DOI: 10.5194/acp-21-13131-2021.

(14) Yadav, V.; Duren, R.; Mueller, K.; Verhulst, K. R.; Nehrkorn, T.; Kim, J.; Weiss, R. F.; Keeling, R.; Sander, S.; Fischer, M. L.; Newman, S.; Falk, M.; Kuwayama, T.; Hopkins, F.; Rafiq, T.; Whetstone, J.; Miller, C. Spatio-temporally Resolved Methane Fluxes From the Los Angeles Megacity. *Journal of Geophysical Research: Atmospheres* **2019**, *124* (9), 5131-5148. DOI: 10.1029/2018jd030062.

(15) Wennberg, P. O.; Mui, W.; Wunch, D.; Kort, E. A.; Blake, D. R.; Atlas, E. L.; Santoni, G. W.; Wofsy, S. C.; Diskin, G. S.; Jeong, S.; Fischer, M. L. On the Sources of Methane to the Los Angeles Atmosphere. *Environ. Sci. Technol.* **2012**, *46* (17), 9282-9289. DOI: 10.1021/es301138y.

(16) Ren, X.; Salmon, O. E.; Hansford, J. R.; Ahn, D.; Hall, D.; Benish, S. E.; Stratton, P. R.; He, H.; Sahu, S.; Grimes, C.; Heimburger, A. M. F.; Martin, C. R.; Cohen, M. D.; Stunder, B.; Salawitch, R. J.; Ehrman, S. H.; Shepson, P. B.; Dickerson, R. R. Methane Emissions From the Baltimore-Washington Area Based on Airborne Observations: Comparison to Emissions Inventories. *Journal of Geophysical Research: Atmospheres* **2018**, *123* (16), 8869-8882. DOI: 10.1029/2018JD028851.

(17) Plant, G.; Kort, E. A.; Floerchinger, C.; Gvakharia, A.; Vimont, I.; Sweeney, C. Large Fugitive Methane Emissions From Urban Centers Along the U.S. East Coast. *Geophysical Research Letters* **2019**, *46* (14), 8500-8507. DOI: 10.1029/2019gl082635.

(18) Huang, Y.; Kort, E. A.; Gourdji, S.; Karion, A.; Mueller, K.; Ware, J. Seasonally Resolved Excess Urban Methane Emissions from the Baltimore/Washington, DC Metropolitan Region. *Environ Sci Technol* **2019**, *53* (19), 11285-11293. DOI: 10.1021/acs.est.9b02782 From NLM Medline.

(19) Lopez-Coto, I.; Ren, X.; Salmon, O. E.; Karion, A.; Shepson, P. B.; Dickerson, R. R.; Stein, A.; Prasad, K.; Whetstone, J. R. Wintertime CO2, CH4, and CO Emissions Estimation for the

Washington, DC–Baltimore Metropolitan Area Using an Inverse Modeling Technique. *Environ. Sci. Technol.* **2020**, *54* (5), 2606-2614. DOI: 10.1021/acs.est.9b06619.

(20) Saint-Vincent, P. M. B.; Pekney, N. J. Beyond-the-Meter: Unaccounted Sources of Methane Emissions in the Natural Gas Distribution Sector. *Environ. Sci. Technol.* **2020**, *54* (1), 39-49. DOI: 10.1021/acs.est.9b04657.

(21) Fischer, M. L.; Chan, W. R.; Delp, W.; Jeong, S.; Rapp, V.; Zhu, Z. An Estimate of Natural Gas Methane Emissions from California Homes. *Environ. Sci. Technol.* **2018**, *52* (17), 10205-10213. DOI: 10.1021/acs.est.8b03217.

(22) Merrin, Z.; Francisco, P. W. Unburned Methane Emissions from Residential Natural Gas Appliances. *Environ. Sci. Technol.* **2019**, *53* (9), 5473-5482. DOI: 10.1021/acs.est.8b05323.

(23) Lebel, E. D.; Finnegan, C. J.; Ouyang, Z.; Jackson, R. B. Methane and NOx Emissions from Natural Gas Stoves, Cooktops, and Ovens in Residential Homes. *Environ. Sci. Technol.* **2022**, *56* (4), 2529-2539. DOI: 10.1021/acs.est.1c04707.

(24) Lebel, E. D.; Lu, H. S.; Speizer, S. A.; Finnegan, C. J.; Jackson, R. B. Quantifying Methane Emissions from Natural Gas Water Heaters. *Environ. Sci. Technol.* **2020**, *54* (9), 5737-5745. DOI: 10.1021/acs.est.9b07189.

(25) EPA. Inventory of U.S. Greenhouse Gas Emissions and Sinks 1990-2020: Updates for Post-Meter Emissions. 2022. https://www.epa.gov/system/files/documents/2022-04/2022_ghgi_update_-_meter.pdf (accessed 2022 November).

(26) Floerchinger, C.; Shepson, P. B.; Hajny, K.; Daube, B. C.; Stirm, B. H.; Sweeney, C.; Wofsy, S. C. Relative flux measurements of biogenic and natural gas-derived methane for seven U.S. cities. *Elementa: Science of the Anthropocene* **2021**, *9* (1). DOI: 10.1525/elementa.2021.000119 (acccessed 12/23/2022).

(27) Zeng, Z.-C.; Pongetti, T.; Newman, S.; Oda, T.; Gurney, K.; Palmer, P. I.; Yung, Y. L.; Sander, S. P. Decadal decrease in Los Angeles methane emissions is much smaller than bottom-up estimates. *Nature Communications* **2023**, *14* (1), 5353. DOI: 10.1038/s41467-023-40964-w.

(28) United States Census. 2010 Census Urban and Rural Classification and Urban Area Criteria. 2010. https://www.census.gov/programs-surveys/geography/guidance/geo-areas/urban-rural/2010-urban-rural.html (accessed 2022 November).

(29) Karion, A.; Callahan, W.; Stock, M.; Prinzivalli, S.; Verhulst, K. R.; Kim, J.; Salameh, P. K.; Lopez-Coto, I.; Whetstone, J. Greenhouse gas observations from the Northeast Corridor tower network. *Earth Syst. Sci. Data* **2020**, *12* (1), 699-717. DOI: 10.5194/essd-12-699-2020.

(30) Karion, A.; DiGangi, E.; Prinzivalli, S.; Draper, C.; Baldelli, S.; Fain, C.; Biggs, B.; Stock, M.; Michalak, B.; Salameh, P.; Kim, J.; Callahan, W.; Whetstone, J. Observations of carbon dioxide (CO2), methane (CH4), and carbon monoxide (CO) mole fractions from the NIST Northeast Corridor urban testbed. National Institute of Standards and Technology, Ed.; 2023. https://doi.org/10.18434/mds2-3012 (accessed May 8 2023).

(31) Lopez-Coto, I.; Ghosh, S.; Prasad, K.; Whetstone, J. Tower-based greenhouse gas measurement network design—The National Institute of Standards and Technology North East Corridor Testbed. *Advances in Atmospheric Sciences* **2017**, *34* (9), 1095-1105, journal article. DOI: 10.1007/s00376-017-6094-6.

(32) Mueller, K.; Yadav, V.; Lopez-Coto, I.; Karion, A.; Gourdji, S.; Martin, C.; Whetstone, J. Siting Background Towers to Characterize Incoming Air for Urban Greenhouse Gas Estimation: A Case Study in the Washington, DC/Baltimore Area. *Journal of Geophysical Research: Atmospheres* **2018**, *123* (5), 2910-2926. DOI: doi:10.1002/2017JD027364.

(33) Karion, A.; Lopez-Coto, I.; Gourdji, S. M.; Mueller, K.; Ghosh, S.; Callahan, W.; Stock, M.; DiGangi, E.; Prinzivalli, S.; Whetstone, J. Background conditions for an urban greenhouse gas network in the Washington, DC, and Baltimore metropolitan region. *Atmos. Chem. Phys.* **2021**, *21* (8), 6257-6273. DOI: 10.5194/acp-21-6257-2021.

(34) Lin, J. C.; Gerbig, C.; Wofsy, S. C.; Andrews, A. E.; Daube, B. C.; Davis, K. J.; Grainger, C. A. A near-field tool for simulating the upstream influence of atmospheric observations: The Stochastic Time-Inverted Lagrangian Transport (STILT) model. *Journal of Geophysical Research: Atmospheres* **2003**, *108* (D16). DOI: https://doi.org/10.1029/2002JD003161.

(35) Hersbach, H.; Bell, B.; Berrisford, P.; Hirahara, S.; Horányi, A.; Muñoz-Sabater, J.; Nicolas, J.; Peubey, C.; Radu, R.; Schepers, D.; Simmons, A.; Soci, C.; Abdalla, S.; Abellan, X.; Balsamo, G.; Bechtold, P.; Biavati, G.; Bidlot, J.; Bonavita, M.; De Chiara, G.; Dahlgren, P.; Dee, D.; Diamantakis, M.; Dragani, R.; Flemming, J.; Forbes, R.; Fuentes, M.; Geer, A.; Haimberger, L.; Healy, S.; Hogan, R. J.; Hólm, E.; Janisková, M.; Keeley, S.; Laloyaux, P.; Lopez, P.; Lupu, C.; Radnoti, G.; de Rosnay, P.; Rozum, I.; Vamborg, F.; Villaume, S.; Thépaut, J.-N. The ERA5 global reanalysis. *Quarterly Journal of the Royal Meteorological Society* **2020**, *146* (730), 1999-2049. DOI: https://doi.org/10.1002/qj.3803.

(36) Skamarock, W. C.; Klemp, J. B.; Dudhia, J.; Gill, D. O.; Liu, Z.; Berner, J.; Wang, W.; Powers, J. G.; Duda, M. G.; Barker, D.; Huang, X.-y. *A Description of the Advanced Research WRF Model Version 4*; No. NCAR/TN-556+STR; National Center for Atmospheric Research, Boulder, CO, 2019.

(37) Pitt, J. R., Lopez-Coto, I., Karion, A., Hajny, K., Tomlin, J., Whetstone, J., Shepson, P. New York City methane emissions: what are we missing? **in prep.**

(38) EPA. Inventory of U.S. Greenhouse Gas Emissions and Sinks: 1990-2020. Agency, U. S. E. P., Ed.; U.S. Environmental Protection Agency: 2022; Vol. EPA 430-R-22-003. https://www.epa.gov/ghgemissions/draft-inventory-us-greenhouse-gas-emissions-and-sinks-1990-2020 (accessed 2022 November).

(39) Weller, Z. D.; Hamburg, S. P.; von Fischer, J. C. A National Estimate of Methane Leakage from Pipeline Mains in Natural Gas Local Distribution Systems. *Environ. Sci. Technol.* **2020**, *54* (14), 8958-8967. DOI: 10.1021/acs.est.0c00437.

(40) EPA. GHG Reporting Program Facility-Level Information on Greenhouse Gases Tool (FLIGHT). 2021. ghgdata.epa.gov/ghgp/main.do (accessed 2022 December 8).

(41) Maasakkers, J. D.; Jacob, D. J.; Sulprizio, M. P.; Turner, A. J.; Weitz, M.; Wirth, T.; Hight, C.; DeFigueiredo, M.; Desai, M.; Schmeltz, R.; Hockstad, L.; Bloom, A. A.; Bowman, K. W.; Jeong, S.; Fischer, M. L. Gridded National Inventory of US Methane Emissions. *Environ. Sci. Technol.* **2016**, *50* (23), 13123-13133, Article. DOI: 10.1021/acs.est.6b02878.

(42) Tarantola, A. *Inverse Problem Theory and Methods for Model Parameter Estimation*; SIAM, 2005.

(43) Energy Information Administration (EIA). Natural Gas Annual Respondent Query System (EIA-176). 2022. https://www.eia.gov/naturalgas/ngqs (accessed 2022 March).

(44) Gurney, K. R.; Liang, J.; Patarasuk, R.; Song, Y.; Huang, J.; Roest, G. The Vulcan Version 3.0 High-Resolution Fossil Fuel CO2 Emissions for the United States. *Journal of Geophysical Research-Atmospheres* **2020**, *125* (19), e2020JD032974. DOI: https://doi.org/10.1029/2020JD032974.

(45) Gurney, K. R.; Liang, J.; Patarasuk, R.; Song, Y.; Huang, J.; Roest, G. Vulcan: High-Resolution Annual Fossil Fuel CO2 Emissions in USA, 2010-2015, Version 3. Gurney, K. R., Liang, J., Patarasuk, R., Song, Y., Huang, J., Roest, G., Eds.; ORNL Distributed Active Archive Center: 2020. https://daac.ornl.gov/cgi-bin/dsviewer.pl?ds_id=1741 (accessed 2020 June).

(46) Energy Information Administration (EIA). Natural Gas Consumption by End Use. https://www.eia.gov/dnav/ng/ng_cons_sum_a_EPG0_vgt_mmcf_m.htm (accessed 2022 February 28).

(47) Lopez-Coto, I.; Ren, X.; Salmon, O. E.; Karion, A.; Shepson, P. B.; Dickerson, R. R.; Stein, A.; Prasad, K. R.; Whetstone, J. Wintertime CO2, CH4 and CO emissions estimation for the Washington DC / Baltimore metropolitan area using an inverse modeling technique. *Environ. Sci. Technol.* **2020**. DOI: 10.1021/acs.est.9b06619.

(48) Mueller, K. L.; Lauvaux, T.; Gurney, K. R.; Roest, G.; Ghosh, S.; Gourdji, S. M.; Karion, A.; DeCola, P.; Whetstone, J. An emerging GHG estimation approach can help cities achieve their climate and sustainability goals. *Environmental Research Letters* **2021**, *16* (8). DOI: ARTN 084003
10.1088/1748-9326/ac0f25.

(49) Spokas, K. A.; Bogner, J.; Corcoran, M. Modeling landfill CH4 emissions: CALMIM international field validation, using CALMIM to simulate management strategies, current and future climate scenarios. *Elementa: Science of the Anthropocene* **2021**, *9* (1). DOI: 10.1525/elementa.2020.00050.

(50) Reddy, K. R.; Rai, R. K.; Green, S. J.; Chetri, J. K. Effect of temperature on methane oxidation and community composition in landfill cover soil. *Journal of Industrial Microbiology and Biotechnology* **2019**, *46* (9-10), 1283-1295. DOI: 10.1007/s10295-019-02217-y (acccessed 6/5/2023).

(51) Cusworth, D. H.; Duren, R. M.; Thorpe, A. K.; Tseng, E.; Thompson, D.; Guha, A.; Newman, S.; Foster, K. T.; Miller, C. E. Using remote sensing to detect, validate, and quantify

methane emissions from California solid waste operations. *Environmental Research Letters* **2020**, *15* (5), 054012. DOI: 10.1088/1748-9326/ab7b99.

(52) Xu, L.; Lin, X.; Amen, J.; Welding, K.; McDermitt, D. Impact of changes in barometric pressure on landfill methane emission. *Global Biogeochemical Cycles* **2014**, *28* (7), 679-695. DOI: https://doi.org/10.1002/2013GB004571.

(53) Vázquez-Lule, A.; Vargas, R. Biophysical drivers of net ecosystem and methane exchange across phenological phases in a tidal salt marsh. *Agricultural and Forest Meteorology* **2021**, *300*, 108309. DOI: https://doi.org/10.1016/j.agrformet.2020.108309.

(54) Liu, Y.; Sharma, K. R.; Fluggen, M.; O'Halloran, K.; Murthy, S.; Yuan, Z. Online dissolved methane and total dissolved sulfide measurement in sewers. *Water Research* **2015**, *68*, 109-118. DOI: https://doi.org/10.1016/j.watres.2014.09.047.

(55) Bloom, A. A.; Bowman, K. W.; Lee, M.; Turner, A. J.; Schroeder, R.; Worden, J. R.; Weidner, R.; McDonald, K. C.; Jacob, D. J. A global wetland methane emissions and uncertainty dataset for atmospheric chemical transport models (WetCHARTs version 1.0). *Geosci. Model Dev.* **2017**, *10* (6), 2141-2156. DOI: 10.5194/gmd-10-2141-2017.

(56) Yadav, V.; Ghosh, S.; Mueller, K.; Karion, A.; Roest, G.; Gourdji, S. M.; Lopez-Coto, I.; Gurney, K. R.; Parazoo, N.; Verhulst, K. R.; Kim, J.; Prinzivalli, S.; Fain, C.; Nehrkorn, T.; Mountain, M.; Keeling, R. F.; Weiss, R. F.; Duren, R.; Miller, C. E.; Whetstone, J. The Impact of COVID-19 on CO2 Emissions in the Los Angeles and Washington DC/Baltimore Metropolitan Areas. *Geophysical Research Letters* **2021**, *48* (11). DOI: 10.1029/2021gl092744.

(57) Montgomery County Council. Bill 13-22 - Buildings – Comprehensive Building Decarbonization. In *13-22*, County Council for Montgomery County, M., Ed.; 2022; Vol. 13-22. https://apps.montgomerycountymd.gov/ccllims/DownloadFilePage?FileName=2754_1_23710_Bill_13-22_Signed_20221212.pdf (accessed 2023 April 6).